Title

Diurnal infection patterns and impact of *Microcystis* cyanophage in a Japanese pond

Running title

Diurnal infection patterns of *Microcystis* cyanophage

Authors

Shigeko Kimura[1], Takashi Yoshida[1#], Naohiko Hosoda[2], Takashi Honda[1], Sotaro Kuno[1], Rikae Kamiji[1], Ryoya Hashimoto[1] and Yoshihiko Sako[1].

Affiliation

[1] Graduate School of Agriculture, Kyoto University, Kitashirakawa-Oiwake, Sakyo-ku, Kyoto 606-8502, Japan

[2] Departmennt of Marine Bioscience, Fukui Prefectural University, 1-1 Gakuen-cho, Obama, Fukui 917-0003, Japan

Corresponding author

Takashi Yoshida

Postal address: Graduate School of Agriculture, Kyoto University, Kitashirakawa-Oiwake, Sakyo-ku, Kyoto 606-8502, Japan. Phone: (+81) 75-753-6218. Fax: (+81) 75-7533-6226. E-mail: yoshiten@kais.kyoto-u.ac.jp

Journal section

Environmental microbiology

Abstract

Viruses play important roles in regulating the abundance, clonal diversity, and composition of their host populations. To assess their impact on the host populations, it is essential to understand the dynamics of virus infections in the natural environment. Cyanophages often carry host-like genes including photosynthesis genes that maintain host photosynthesis. This implies a diurnal pattern of cyanophage infection depending on photosynthesis. Here, we investigated the infection pattern of *Microcystis* cyanophage by following the abundances of Ma-LMM01-type phage tail sheath *g91* gene and its transcript in a natural population. The relative *g91* mRNA abundance within host cells showed a peak during the daylight hours and was lowest around midnight. The phage *g91* DNA copy numbers in host cell fractions, which are predicted to indicate phage replications, increased in the afternoon, followed by an increase in the free phage fractions. In all fractions at least one of 71 *g91* genotypes was observed (in tested host cell, free phage and RNA fractions), indicating the replication cycle of the cyanophage was occurring (i.e. injection, transcription, replication, and release of progeny phages). Thus, *Microcystis* cyanophage infection occurs in a diel cycle, which may depend on the light cycle. Additionally, our data shows the abundance of

45 mature cyanophage produced within host cells was 1-2 orders of magnitude greater
46 than released phages, suggesting phage production may be higher than previously
47 reported.
48

Introduction

Viruses play important roles in regulating the abundance, clonal diversity and composition of cyanobacterial populations, and thus have potential impact on the biogeochemical cycles through the process of virus-mediated cell lysis (21, 37). To assess their impacts on the host, the frequency of infected host cells is often estimated from viral production, which is calculated from measurements of viral abundance (10, 12, 44, 46). However, previous studies show viral abundance vary hour-to-hour and day-to-day (45). Therefore, it is essential to understand viral infection dynamics to determine the impact of the virus on host populations.

Marine cyanophages infecting cyanobacteria *Prochlorococcus* and *Synechococcus*, which contribute significantly to the primary production of the open ocean, often carry host-like genes involved in photosynthesis, the pentose phosphate pathway, and carbon metabolism (26, 33-35). Recent studies show these genes direct carbon flux from the Calvin cycle to the pentose phosphate pathway, suggesting the phage augments production of energy (ATP) and reducing power (NADPH) to fuel phage dNTP biosynthesis (1, 41).

Ma-LMM01 is a lytic myovirus infecting a strain of *Microcystis aeruginosa* that frequently forms noxious cyanobacterial blooms in eutrophic freshwater

environments (50). The majority of predicted genes in its genome have no detectable homologues in the present databases and thus Ma-LMM01 was assigned as a member of a new lineage of the Myoviridae family (5, 49). In contrast to the marine cyanophages possessing photosynthetic genes, Ma-LMM01 possesses a homologue of the *nblA* gene that plays a central role in the degradation of phycobilisomes. *M. aeruginosa* has a gas vacuole conferring it buoyancy to float near surface waters where *M. aeruginosa* are exposed to high light intensity, which may rapidly lead to photo-inhibition upon phage infection. Recently, a second example of cyanophage-encoded *nblA* was found in a phage infecting freshwater cyanobacterium *Planktothrix agardhii* that has a gas vacuole (9). Phage *nblA* gene is predicted to function by maintaining host photosynthesis (49). This led to the hypothesis that cyanophage infection may have a diurnal pattern dependent on photosynthesis (36). Further, the latent period of Ma-LMM01 is from 6 to 12 hours (50), suggesting the length of lytic cycle fits in the daylight. However, little is known about the cyanophage infection cycle associated with the light cycle in natural populations.

Synechococcus cyanophage abundance was previously determined using the plaque assay on solid medium and the most probable number (MPN) method using

Synechococcus isolates (38). However, it was considered the culture-based methods often underestimate the abundances where the quantifiable cyanophage is limited to the cyanophages that infect only laboratory isolates of *Synechococcus* (25). One approach to avoid this problem is to use a PCR based method (29, 32). Similarly, we have never been detected *Microcystis* cyanophage using culture-dependent methods with several host strains (40). Therefore, to determine if cyanophage infections have diurnal patterns associated with the light cycle, we monitored the abundance of a *M. aeruginosa*-infectious cyanophage gene and its transcripts using real-time PCR during 24 h in a Japanese freshwater pond.

Materials and Methods

Study site and Sampling. Diel changes of *Microcystis aeruginosa* and its cyanophages were investigated at Hirosawanoike Pond (35º02' N, 135º41' E), Japan, a small (surface area: 14 ha) and shallow (mean depth: 1.5 m) reservoir in the form of a farm pond. Hirosawanoike Pond receives high nutrient input in relation to its volume due to raising carp agriculturally. This results in eutrophication and cyanobacterial blooms from early summer to autumn every year (48). Water samples of surface water were taken from a boat every 3 h over a period of 24 h on

15 to 16 Sep and on 21 to 22 Oct 2009 at a fixed point in the pond. Two liters of pond water were stored in brown bottles and transported to the laboratory within 1h. For DNA extraction, water samples were separated into a free phage and a host cell fraction. For preparation of the free phage fractions, 10 mL of the pond water was filtered using a 0.2 μm polycarbonate filter. Recovery of phage particles with this procedure was 65.1 % using a lysate of Ma-LMM01-infected *M. aeruginosa* NIES298 cells. The 0.2 μm filtrates were ultra-centrifuged at 111,000 × *g* for 1.5 h at 4 ˚C (40). The pellet was re-suspended in 200 μL deionized water and stored at -80 ˚C. For the host cell fractions, 100 mL of the pond water was sonicated gently and harvested using centrifugation at 1,680 × *g* for 10 min (51). The pellet was stored at -20 ˚C until DNA analysis. For the transcriptional analysis of phage mRNA, 20 to 100 mL of the sample was collected on a 3-μm PTFE membrane filter (a RNA fraction) and re-suspended in 1 mL of Stop Solution (TE-saturated phenol:ethanol=5:95 [v/v]) according to Yoshida *et al*. (2010). The suspension was stored at -20 °C. We extracted DNA and RNA within three months.

A seasonal study of variations in *M. aeruginosa* and its cyanophages was performed at the same sampling site in the diel study from 21 Apr to 17 Nov 2009 once per month. Seasonal samples were treated the same as samples for the diel

study described above.

DNA extraction. DNA extraction from host cell fractions was performed using the xanthogenate method as described previously (51). DNA extraction from free viral fractions was performed as previously described (40). To avoid contamination with dissolved DNA, the filtrate was treated with DNase I at 37 $^{\circ}$C for 1 h before DNA extraction. Purified DNAs were suspended in 30 µL deionized water. The amount and purity of the extracted DNA were determined using optical density comparison at 260 nm and 280 nm. Each DNA extract was used as the template for real-time PCR to quantify the abundances of total *M. aeruginosa* and its infectious cyanophages.

RNA extraction, purification and cDNA synthesis. Total RNA was extracted from 1 ml of the stored cell suspension as described previously (48). The purified RNA was suspended in 30 µL of dimethyl dicarbonate (DMDC)-treated water. The amount and purity of the extracted RNA were determined using optical density comparison at 260 nm and 280 nm. After digestion with DNase I, 1 µg of purified RNA was reverse transcribed using random primers with the SuperScriptIII

first-strand synthesis system (Invitrogen) according to the manufacturer's instructions. Each cDNA was used as the template for real-time RT-PCR to quantify cyanophage mRNA.

Real-time PCR and Real-time RT-PCR amplification. To quantify abundances of total *M. aeruginosa* and its infectious cyanophages, a real-time PCR assay was performed using primers based on sequences of the phycocyanin intergenic spacer (PC-IGS) gene and the Ma-LMM01 tail sheath gene *g91*, respectively, as described previously (48). The primer pairs used; 188F-254R (16) and sheathRTF-SheathRTR (40) are shown in Table S1. The numbers of *g91* DNA gene were studied in two fractions; the host cell fraction and the free phage fraction. To detect related cyanophage mRNA, we performed a real-time RT-PCR with the primer sets SheathRTF-SheathRTR and rnpbRTF-rnpbRTR targeting the cyanophage *g91* and RNase P RNA gene (*rnpB*) of *M. aeruginosa*, respectively (Table S1). To normalize the raw expression levels of the phage *g91* mRNA, the relative abundance of *g91* was compared to the *rnpB* gene transcripts of the host *M. aeruginosa*. A minimum of three replicates was used to quantify numbers. Real-time PCR and real-time RT-PCR were performed with 1 µl of each extracted DNA using

157 SYBR® *Premix Ex Taq*™. Individual real-time PCR was performed for each primer
158 set according to the following cycle parameters: for *M. aeruginosa* (PC-IGS):
159 denaturation at 95 °C for 15 sec, annealing at 60 °C for 15 sec, and extension at 72
160 °C for 30 sec; for its infectious cyanophages (*g91*): denaturation at 95 °C for 15 sec,
161 annealing at 58 °C for 15 sec, and extension at 80 °C for 30 sec; and for RNase P
162 RNA gene (*rnpB*): denaturation at 95 °C for 15 sec, annealing at 58 °C for 15 sec,
163 and extension at 78°C for 30 sec.

164 Real-time PCR products of *g91* genes were cloned into the pGEM-T Easy vector
165 (Promega) and then transformed into *E. coli* INVαF'-competent cells (Invitrogen)
166 according to the manufacturer's instructions. At least 20 positive clones (white
167 colonies) from each clone library were randomly selected and then sequenced at
168 the Dragon Genomics Center, Takara Bio, Inc. (Otsu, Japan).

169

170 **Primer design for *g91* clonal analysis using TAIL-PCR, PCR amplification, and**
171 **Sequencing.** We designed a new degenerate primer set (g91F and g91R) to
172 access genetic relationships among *g91* genes in both fractions and the transcripts
173 with a *g91* clonal analysis because *g91* real-time PCR products are too short (136
174 bp). As no strain closely related to Ma-LMM01 has been isolated, the degenerate

175 primer set (g91F and g91R) was designed based on sequences obtained using a
176 combination of real-time PCR products with thermal asymmetric interlaced
177 (TAIL)-PCR products from environmental samples.

178 First, we determined the downstream flanking sequences of *g91* real-time PCR
179 products using TAIL-PCR with three specific primers (SheathTPF1-3) designed
180 based on the sequence of Ma-LMM01 *g91* and eight arbitrary (AD1-8) primer sets
181 (Table S1, Fig 1) (19, 20). Reaction conditions for the TAIL-PCR were as described
182 previously (15). The sheathTPF2 and AD2, 4, 5, and 7 primer sets had amplified
183 products (1 to 1.5-kbp fragments) from all of the three fractions in environmental
184 samples from Hirosawanoike Pond. The PCR products with the sheathTPF2-AD2
185 primer set were purified using a Wizard Miniprep Purrification Kit (Promega,
186 Madison, WI, USA), cloned into pTAC-1 or pTAC-2 Vectors (BioDynamics) and then
187 transformed into *E. coli* DH5α-competent cells. Ten positive clones (white colonies)
188 from each clone library were randomly selected and sequenced using a 3130
189 Genetic Analyzer (Applied Biosystems, Foster City, CA, USA) with a BigDye
190 Terminator v3.1 Cycle Sequencing Kit according to the manufacturer's instructions
191 (Applied Biosystems, Foster City, CA, USA). The reverse primer g91R was
192 designed manually comparing the variable regions of sequence alignment of

193 SheathTPF2-AD2 amplified products from the three fractions. In addition, we
194 designed the forward primer g91F against variable regions of *g91* real-time
195 products from the three fractions (Fig. 1, Table S1).

196 PCR amplification with primer sets g91F and g91R was performed in a total
197 volume of 25 μl containing 10×*Ex Taq* Buffer, 200 μM dNTP mix, 0.5 μM each primer,
198 1.25U TaKaRa *Ex Taq*^{TM} polymerase, and 1 μl of each DNA template. The reaction
199 conditions were an initial denaturation at 94 $^{\circ}$C for 3 min, followed by 30 cycles of
200 denaturation at 94 $^{\circ}$C for 30 sec, annealing at 58 $^{\circ}$C for 30 sec, and extension at 72
201 $^{\circ}$C for 1.5 min, with a final extension at 72 $^{\circ}$C for 10 min. The PCR products were
202 purified, cloned and sequenced as described above. Maximum parsimony network
203 analysis was performed using the statistical parsimony program TCS v1.21 (7).

204

205 **Nucleotide Sequence.** The nucleotide sequences determined in this study are
206 deposited in the DDBJ/EMBL/GenBank database. The accession numbers are as
207 follows: AB690464 to AB690490 for clones of *g91* arrays from the host cell fraction,
208 and AB690491 to AB690520 for *g91* arrays from the RNA fraction, and AB690521 to
209 AB690550 for *g91* arrays from the free phage fraction.

210

211 **Results**

212 **Population dynamics of *M. aeruginosa*.** We performed 24-hour sampling on
213 15-16 Sep and 20-21 Oct of 2009. Hereafter, we refer to these samplings as the first
214 sampling and the second sampling, respectively. In the first sampling, the PC-IGS
215 gene copy numbers of *M. aeruginosa* were nearly constant at approximately 10^6
216 copies ml^{-1} from 09:00 to 00:00 and increased at 03:00 and then declined to the
217 same level (4.9×10^6 copies mL^{-1}) as in the beginning sample (Fig. 2). The 3:00 peak
218 resulted from an accumulation of *M. aeruginosa* in the surface water caused by a
219 well-known diel vertical migration by *M. aeruginosa* (30, 43). The PC-IGS gene copy
220 numbers in the second sampling also showed a pattern similar to that of the first
221 (Fig. 2).

222

223 **Diel infection dynamics of *Microcystis* cyanophage.** We monitored the
224 abundance of *g91* DNA copy numbers in the free phage fraction as well as the host
225 cell fraction. A putative site-specific recombinase gene was found in the Ma-LMM01
226 genome (49). However, this gene has been re-annotated as a variant of the IS607
227 family members not related to lysogeny (15). Further, no amplicon is observed from
228 the isolated 29 cyanobacterial strains using *g91*-targeted PCR (40). This suggests

229 the Ma-LMM01-type phage is a virulent phage and the *g91* gene in the host cell
230 fraction is not replicated with the host genome as a prophage, but is newly
231 replicated using host machinery immediately after infection. The gene copy
232 numbers in the host cell fraction may be predicted as a marker to evaluate phage
233 replication. We also monitored the diurnal pattern of cyanophage gene expression.
234 In the first sampling, the phage *g91* DNA copy numbers in the free phage fraction
235 were 1.3×10^{2} copies mL^{-1} at 09:00, the initial sampling time, and then showed a
236 peak at 3.9×10^{2} copies mL^{-1} from 15:00 to 18:00 (Fig. 3A). The phage *g91* DNA
237 copy numbers in the host cell fraction were much higher than those in the free
238 phage fraction (Fig. 3A and B). The phage copy numbers in the host cell fraction
239 were 1.5×10^{4} copies mL^{-1} at 09:00, and subsequently increased to 1.3×10^{5} copies
240 mL^{-1} at 15:00 and then decreased to 5.2×10^{3} copies mL^{-1} at 21:00 (Fig. 3B). The
241 relative abundance of the cyanophage *g91* mRNA was 0.0026 at 09:00, and then
242 showed a peak (0.0051) at 12:00 and its lowest relative abundance (0.0007) at
243 03:00 in the first sampling (Fig. 3C). In the second sampling, the phage *g91* DNA
244 copy numbers in the free phage fraction showed a first peak (2.2×10^{3} copies mL^{-1})
245 at 21:00; decreased to 1.3×10^{2} copies mL^{-1} at 00:00; and then showed a second
246 peak at 1.5×10^{3} copies mL^{-1} from 03:00 to 06:00 (Fig. 3D). Phage *g91* DNA copy

numbers in the host cell fraction were 2.6×10^4 copies mL^{-1} at 09:00 and subsequently had a first peak at 1.2×10^5 copies mL^{-1} from 12:00 to 15:00 (inset in Fig. 3E) and then a second peak at 1.1×10^6 copies mL^{-1} at 03:00 (Fig. 3E). The *g91* transcripts in the second sampling showed the same trend as dynamics observed in the first sampling (Fig. 3F), suggesting that the first peak in *g91* DNA copy numbers in both fractions was derived from phage production; and the 03:00 peak in phage *g91* DNA copy numbers in both fractions at the second sampling was associated with *M. aeruginosa* accumulating at the water surface during the night rather than with phage proliferation in host cells since the transcripts showed the lowest value at 03:00.

The relationship between *g91* genotypes in all of the three fractions. Next, we accessed genetic relationships among *g91* sequences in three fractions (host DNA, viral DNA and host transcripts). Given that a type of phage inject their DNA into cells of a host population, replicate their DNA within the cells, and release their progenies into the environment, we would obtain sequences identical to the phage *g91* sequence from all the fractions. Twenty-seven, 30, and 30 clones were sequenced from the host cell, the free phage, and the RNA fractions of the first sampling,

265 respectively. When searched against the NCBI non-redundant protein sequence
266 database using BLAST, all the sequences showed significant similarities to only the
267 corresponding region of Ma-LMM01 *g91* (data not shown). The eighty-seven
268 sequences were assigned as 71 genotypes (G1-G71) clustered at 100 % nucleotide
269 sequence identity.

270 To determine relationships between the 71 different phage *g91* genotypes and
271 Ma-LMM01, we conducted a maximum parsimony network analysis. This network
272 showed the genotypes were largely divided into three sequence groups: g91-1,
273 g91-2 and g91-3 groups consisting of 62, 7 and 2 genotypes, respectively; and
274 these groups were genetically distinct from Ma-LMM01 (Fig. 4). Comparing the
275 sequences of the representatives from the three groups (G1, g91-1 group; G25,
276 g91-2 group; G57, g91-3 group), nucleotide differences between each pair were 15
277 (1.3 %, G1 and G25), 60 (5.4 %, G1 and G57), and 55 (4.9 %, G25 and G57). The
278 G1 type which was the predominant group g91-1 genotype was found in all of the
279 three fractions. Twenty-nine, 15, and 13 genotypes of the group g91-1 differed from
280 G1 type by 1, 2, and 3 nucleotides, respectively. Except for one genotype,
281 sequences of the g91-2 group were only found in the RNA fraction.

282

283 **Seasonal dynamics of *M. aeruginosa* and cyanophage in the host cell fraction**
284 **and in the free phage fraction.** The PC-IGS gene copy numbers of *M. aeruginosa*
285 were between 6.1×10^{4} and 3.9×10^{7} copies mL^{-1} from Apr to Nov in 2009 (Fig. 5).
286 The cyanophage *g91* DNA copy numbers in the free phage fraction ranged from
287 below the detection limit to 8.2×10^{2} copies mL^{-1}, and those in the host cell fraction
288 were between 2.5×10^{1} and 1.6×10^{6} copies mL^{-1} during this sampling period.
289 Throughout this year, the cyanophage *g91* DNA copy numbers in the host cell
290 fraction were 3–10^{4} times higher than those of a free phage fraction. The phage
291 abundance fluctuates with the host abundance (Fig.5). This trend was also found in
292 the relationship between the free phages and their hosts in previous studies (38, 48).
293 This suggests a portion of the host population is always infected with the phages
294 albeit with diversity in the hosts and the phages (38).
295
296 **Discussion**
297 **Infection cycle of *Microcystis* cyanophage.** Recent reports show cyanophage
298 production depends on host photosynthesis and occurs with a diurnal pattern in
299 laboratory experiments where production of the cyanophage is suppressed
300 completely or reduced by darkness or photosynthetic inhibitors (2, 18, 22); and is

301 correlated with the amount of light that is shown in a diurnal pattern under natural
302 light (13) using laboratory conditions. One field survey concerning infection patterns
303 of natural populations demonstrated *Synechococcus* cyanophage numbers
304 increase at mid-night (8). Therefore, this is a first report describing the diurnal
305 infection patterns of cyanophage depending on the light cycle by determining the
306 dynamics of phage gene replication and transcription in a natural population.

307 Previously, our culture-based data demonstrated that the relative abundance of
308 *g91* gene showed a rapid increase at 1 h post-infection reaching a maximum (10^{-1})
309 at 6 h post-infection (48). Thus, we suggested the relative abundance of the *g91*
310 gene may be a potential marker for environmental monitoring of cyanophage
311 infection. In the field survey reported here, the relative *g91* mRNA abundance
312 showed a peak during daylight and the lowest value around midnight (Fig.3 C and
313 F), thus the expression clearly showed a diurnal pattern. Subsequently, the phage
314 *g91* DNA copy numbers in the host cell fraction increased at 6 (12:00) to 9 (15:00) h
315 after dawn (Fig. 3B and E), which is compatible with the latent period of the
316 cyanophage Ma-LMM01 (6 to 12 h under laboratory conditions) (50); this was
317 followed by an increase in *g91* DNA copy numbers in the free phage fraction (Fig.
318 3A and D). One genotype (G1 type) of *g91* sequences was observed in all three

319 fractions. These patterns suggest the phage genes were transcribed at the
320 beginning of the host's photosynthesis at dawn; then after 6 - 9 hours, mature
321 phages were formed and released from host cells. This suggests *Microcystis*
322 cyanophage proliferation may be dependent on host photosynthetic performance
323 associated with the light cycle and cyanophage infection occurs in a diel cycle.

324 Previously, we demonstrated Ma-LMM01-type cyanophage dynamics may affect
325 shifts of composition of *M. aeruginosa* populations (e.g. microcystin-producing and
326 non-microcystin producing population) during bloom succession (47). The diurnal
327 nature of cyanophage infection implies this shift is produced by accumulation of
328 small changes thorough the 'day-to-day infections'. As pointed out by Winter *et al*.
329 (46), our data also shows that phage production and cell lysis are not held based on
330 a steady-state assumption; therefore, estimates of infected cells calculated from
331 cyanophage abundances necessary to assess the impact of cyanophage on their
332 host population depend on the sampling time.

333 Of 62 genotypes belonging to the g91-1 group, 17 genotypes had silent mutations
334 compared to the G1 type sequence (Fig. 4). A previous study showed the
335 divergence in the phage sequences is derived from point mutations where the
336 majority (>90 %) were silent mutations (28). In contrast, our result shows most

mutations (45/62) result in amino acid changes. This may imply structural plasticity in G91 function is not limited by amino acid changes.

Bacteria have evolved phage defense mechanisms, e.g. the restriction-modification (RM) system, the CRISPR-Cas system, and the abortive infection (Abi) system (17). A recent report shows that the *Microcystis* genome (NIES843) contains a large number of these defense genes (n=492) among the 1,055 bacterial and archael genomes (23), although the presence of these genes in natural populations of *M. aeruginosa* is not addressed. Therefore, it may be likely that the cyanophage genetic variation observed in this study reflects the continuous arms race between the phage and host populations. Further, eight sequences of g91-2 group (9 sequences) were obtained only in the RNA fraction (Fig. 4). One possible explanation is DNA replication of cyanophages included in the g91-2 group may be prevented by one of numerous defense genes including the Abi systems newly identified in *M. aeruginosa* (23) similar to the *AbiK* of Lactococci Abi systems (6).

Impact of *Microcystis* cyanophages on *M. aeruginosa*. The phage *g91* DNA copy numbers in the free phage fraction were 2-3 orders of magnitude lower than

355 those in the host cell fraction when compared at the same sampling time. We
356 observed this trend throughout the year (Fig. 5). Although the packaging efficiency
357 of lytic cyanophage Ma-LMM01 remains unknown, as much as 10-100% of the input
358 DNA is packaged under carefully optimized reaction conditions in a study of T4
359 phage DNA packaging (3, 14, 31). Given the packaging ratio of Ma-LMM01 is 10 %,
360 the abundance of mature cyanophage calculated from the gene abundance in the
361 host cell fraction was still 1-2 orders of magnitude higher than that of free phages.
362 Therefore, phage production estimated from mature phage abundance may be
363 higher than reported previously based on free phage abundance. We speculate
364 some explanations for this large discrepancy: 1) Most progeny phages may be
365 trapped by host lysate or colonies, and small portion diffused gradually into the
366 pond water. 2) Progeny phages may attach to the next hosts for infection or on
367 non-specific particles immediately after diffusing into the pond water. Several
368 authors suggested adsorption on transparent exopolymeric particles may be
369 considered the primary causative agent responsible for removal of viral production
370 in eutrophic reservoirs (4, 27). 3) Progeny phages released into the pond water may
371 be rapidly degraded by UV radiation (10). 4) Infected cells may be preyed upon by
372 protozoa (e.g., heterotrophic nanoflagellates) resulting in decreased numbers of

373 cyanophage released into the pond (24, 39).

374 Our real-time PCR based method may detect small portions of the *Microcystis*
375 cyanophages (i.e. close relatives of Ma-LMM01-type phage) because of specificity
376 of the PCR method. Indeed, previous studies imply there are diverse *Microcytis*
377 cyanophages in the natural environment (11, 42). To quantitatively evaluate the
378 *Microcystis* cyanophage impacts on their host cells, further studies of unkown
379 *Microcystis* cyanophage and the multiple host–phage interactions will be necessary.

380

381 **Acknowledgments**

382 This study was partially supported by Grant-in-Aid for Scientific Research (B) (No.
383 20310045) and JSPS Research Fellowships for Young Scientists (No. 233313).

384 We thank Mr. and Mrs. Matsui for helpful sampling.

385

386 **References**

387 1. **Alperovitch-Lavy A, Sharon I, Rohwer F, Aro EM, Glaser F, Milo R,**
388 **Nelson N, and Beja O.** 2011. Reconstructing a puzzle: existence of
389 cyanophages containing both photosystem-I and photosystem-II gene suites
390 inferred from oceanic metagenomic datasets. Environ Microbiol **13:**24-32.

2. **Benson R, and Martin E.** 1981. Effects of photosynthetic inhibitors and light-dark regimes on the replication of cyanophage SM-2. Arch Microbiol **129:**165-167.

3. **Black LW, and Peng G.** 2006. Mechanistic coupling of bacteriophage T4 DNA packaging to components of the replication-dependent late transcription machinery. J Biol Chem **281:**25635-43.

4. **Bongiorni L, Magagnini M, Armeni M, Noble R, and Danovaro R.** 2005. Viral production, decay rates, and life strategies along a trophic gradient in the North Adriatic Sea. Appl Environ Microbiol **71:**6644-50.

5. **Carstens EB.** 2010. Ratification vote on taxonomic proposals to the International Committee on Taxonomy of Viruses (2009). Arch Virol **155:**133-46.

6. **Chopin MC, Chopin A, and Bidnenko E.** 2005. Phage abortive infection in lactococci: variations on a theme. Curr Opin Microbiol **8:**473-9.

7. **Clement M, Posada D, and Crandall KA.** 2000. TCS: a computer program to estimate gene genealogies. Mol Ecol **9:**1657-9.

8. **Clokie MRJ, Millard AD, Mehta JY, and Mann NH.** 2006. Virus isolation studies suggest short-term variations in abundance in natural cyanophage

populations of the Indian Ocean. J Mar Biol Ass UK **86:**499-505.

9. **Gao EB, Gui JF, and Zhang QY.** 2011. A novel cyanophage with a cyanobacterial nonbleaching protein a gene in the genome. J Virol **86:**236-245.

10. **Garza DR, and Suttle CA.** 1998. The effect of cyanophages on the mortality of *Synechococcus* spp. and selection for UV resistant viral communities. Microb Ecol **36:**281-292.

11. **Honjo M, Matsui K, Ueki M, Nakamura R, Fuhrman JA, and Kawabata Z.** 2006. Diversity of virus-like agents killing *Microcystis aeruginosa* in a hyper-eutrophic pond. J Plankton Res **28:**407-412.

12. **Jiang SC, and Paul JH.** 1994. Seasonal and diel abundance of viruses and occurrence of lysogeny/bacteriocinogeny in the marine-environment. Mar Ecol Prog Ser **104:**163-172.

13. **Kao CC, Green S, Stein B, and Golden SS.** 2005. Diel infection of a cyanobacterium by a contractile bacteriophage. Appl Environ Microbiol **71:**4276-9.

14. **Kondabagil KR, Zhang Z, and Rao VB.** 2006. The DNA translocating ATPase of bacteriophage T4 packaging motor. J Mol Biol **363:**786-99.

15. **Kuno S, Yoshida T, Kamikawa R, Hosoda N, and Sako Y.** 2010. The distribution of a phage-related insertion sequence element in the cyanobacterium, *Microcystis aeruginosa*. Microbes Environ **25:**295-301.

16. **Kurmayer R, and Kutzenberger T.** 2003. Application of real-time PCR for quantification of microcystin genotypes in a population of the toxic cyanobacterium *Microcystis* sp. Appl Environ Microbiol **69:**6723-30.

17. **Labrie SJ, Samson JE, and Moineau S.** 2010. Bacteriophage resistance mechanisms. Nat Rev Microbiol **8:**317-27.

18. **Lindell D, Jaffe JD, Johnson ZI, Church GM, and Chisholm SW.** 2005. Photosynthesis genes in marine viruses yield proteins during host infection. Nature **438:**86-89.

19. **Liu YG, Mitsukawa N, Oosumi T, and Whittier RF.** 1995. Efficient isolation and mapping of *Arabidopsis thaliana* T-DNA insert junctions by thermal asymmetric interlaced PCR. Plant J **8:**457-463.

20. **Liu YG, and Whittier RF.** 1995. Thermal asymmetric interlaced PCR: automatable amplification and sequencing of insert end fragments from P1 and YAC clones for chromosome walking. Genomics **25:**674-681.

21. **Mühling M, Fuller NJ, Millard A, Somerfield PJ, Marie D, Wilson WH,**

Scanlan DJ, Post AF, Joint I, and Mann NH. 2005. Genetic diversity of marine *Synechococcus* and co-occurring cyanophage communities: evidence for viral control of phytoplankton. Environ Microbiol **7:**499-508.

22. **Mackenzie JJ, and Haselkorn R.** 1972. Photosynthesis and the development of blue-green algal virus SM-1. Virology **49:**517-21.

23. **Makarova KS, Wolf YI, Snir S, and Koonin EV.** 2011. Defense islands in bacterial and archaeal genomes and prediction of novel defense systems. J Bacteriol **193:**6039-6056.

24. **Manage PM, Kawabata Z, Nakano S, and Nishibe Y.** 2002. Effect of heterotrophic nanoflagellates on the loss of virus-like particles in pond water. Ecol Res **17:**473-479.

25. **Mann NH.** 2003. Phages of the marine cyanobacterial picophytoplankton. FEMS Microbiol Rev **27:**17-34.

26. **Mann NH, Cook A, Millard A, Bailey S, and Clokie M.** 2003. Bacterial photosynthesis genes in a virus. Nature **424:**741.

27. **Mari X, Kerros ME, and Weinbauer MG.** 2007. Virus attachment to transparent exopolymeric particles along trophic gradients in the southwestern lagoon of New Caledonia. Appl Environ Microbiol **73:**5245-52.

28. **Marston MF, and Amrich CG.** 2009. Recombination and microdiversity in coastal marine cyanophages. Environ Microbiol **11:**2893-2903.

29. **Matteson AR, Loar SN, Bourbonniere RA, and Wilhelm SW.** 2011. Molecular Enumeration of an Ecologically Important Cyanophage in a Laurentian Great Lake. Appl Environ Microbiol **77:**6772-6779.

30. **Reynolds CS, Oliver RL, and Walsby AE.** 1987. Cyanobacterial dominance - the role of buoyancy regulation in dynamic lake environments. N Z J Mar Freshwater Res **21:**379-390.

31. **Sabanayagam CR, Oram M, Lakowicz JR, and Black LW.** 2007. Viral DNA packaging studied by fluorescence correlation spectroscopy. Biophys J **93:**17-9.

32. **Sandaa RA, and Larsen A.** 2006. Seasonal variations in virus-host populations in Norwegian coastal waters: Focusing on the cyanophage community infecting marine *Synechococcus* spp. Appl Environ Microbiol **72:**4610-4618.

33. **Sharon I, Alperovitch A, Rohwer F, Haynes M, Glaser F, Atamna-Ismaeel N, Pinter RY, Partensky F, Koonin EV, Wolf YI, Nelson N, and Beja O.** 2009. Photosystem I gene cassettes are present in marine

virus genomes. Nature **461:**258-262.

34. **Sullivan MB, Huang KH, Ignacio-Espinoza JC, Berlin AM, Kelly L, Weigele PR, DeFrancesco AS, Kern SE, Thompson LR, Young S, Yandava C, Fu R, Krastins B, Chase M, Sarracino D, Osburne MS, Henn MR, and Chisholm SW.** 2010. Genomic analysis of oceanic cyanobacterial myoviruses compared with T4-like myoviruses from diverse hosts and environments. Environ Microbiol **12:**3035-56.

35. **Sullivan MB, Lindell D, Lee JA, Thompson LR, Bielawski JP, and Chisholm SW.** 2006. Prevalence and evolution of core photosystem II genes in marine cyanobacterial viruses and their hosts. PLoS Biol **4:**1344-1357.

36. **Suttle CA.** 2000. Ecological, evolutionary, and geochemical consequences of viral infection of cyanobacteria and eukaryotic algae, p. 247-296. *In* C. J. Hurst (ed.), Viral ecology, Academic Press, San Diego, CA.

37. **Suttle CA.** 2007. Marine viruses - major players in the global ecosystem. Nat Rev Microbiol **5:**801-812.

38. **Suttle CA, and Chan AM.** 1994. Dynamics and distribution of cyanophages and their effect on marine *Synechococcus* spp. Appl Environ Microbiol **60:**3167-3174.

499 39. **Suttle CA, and Chen F.** 1992. Mechanisms and rates of decay of marine
500 viruses in seawater. Appl Environ Microbiol **58:**3721-9.
501 40. **Takashima Y, Yoshida T, Yoshida M, Shirai Y, Tomaru Y, Takao Y,**
502 **Hiroishi S, and Nagasaki K.** 2007. Development and application of
503 quantitative detection of cyanophages phylogenetically related to
504 cyanophage Ma-LMM01 infecting *Microcystis aeruginosa* in fresh water.
505 Microbes Environ **22:**207-213.
506 41. **Thompson LR, Zeng Q, Kelly L, Huang KH, Singer AU, Stubbe J, and**
507 **Chisholm SW.** 2011. Phage auxiliary metabolic genes and the redirection of
508 cyanobacterial host carbon metabolism. Proc Natl Acad Sci U S A
509 **108:**E757-E764.
510 42. **Tucker S, and Pollard P.** 2005. Identification of cyanophage Ma-LBP and
511 infection of the cyanobacterium *Microcystis aeruginosa* from an Australian
512 subtropical lake by the virus. Appl Environ Microbiol **71:**629-635.
513 43. **van Rijn J, and Shilo M.** 1985. Carbohydrate fluctuations, gas vacuolation,
514 and vertical migration of scum-forming cyanobacteria in fishponds. Limnol
515 Oceanogr **30:**1219-1228.
516 44. **Wilhelm SW, Brigden SM, and Suttle CA.** 2002. A dilution technique for the

517 direct measurement of viral production: A comparison in stratified and tidally
518 mixed coastal waters. Microb Ecol **43:**168-173.
519 45. **Winget DM, and Wommack KE.** 2009. Diel and daily fluctuations in
520 virioplankton production in coastal ecosystems. Environ Microbiol
521 **11:**2904-14.
522 46. **Winter C, Herndl GJ, and Weinbauer MG.** 2004. Diel cycles in viral
523 infection of bacterioplankton in the North Sea. Aquat Microb Ecol
524 **35:**207-216.
525 47. **Yoshida M, Yoshida T, Kashima A, Takashima Y, Hosoda N, Nagasaki K,**
526 **and Hiroishi S.** 2008. Ecological dynamics of the toxic bloom-forming
527 cyanobacterium *Microcystis aeruginosa* and its cyanophages in freshwater.
528 Appl Environ Microbiol **74:**3269-3273.
529 48. **Yoshida M, Yoshida T, Yoshida-Takashima Y, Kashima A, and Hiroishi**
530 **S.** 2010. Real-time PCR detection of host-mediated cyanophage gene
531 transcripts during infection of a natural *Microcystis aeruginosa* population.
532 Microbes Environ **25:**211-5.
533 49. **Yoshida T, Nagasaki K, Takashima Y, Shirai Y, Tomaru Y, Takao Y,**
534 **Sakamoto S, Hiroishi S, and Ogata H.** 2008. Ma-LMM01 infecting toxic

Microcystis aeruginosa illuminates diverse cyanophage genome strategies. J Bacteriol **190:**1762-1772.

50. **Yoshida T, Takashima Y, Tomaru Y, Shirai Y, Takao Y, Hiroishi S, and Nagasaki K.** 2006. Isolation and characterization of a cyanophage infecting the toxic cyanobacterium *Microcystis aeruginosa*. Appl Environ Microbiol **72:**1239-1247.

51. **Yoshida T, Yuki Y, Lei S, Chinen H, Yoshida M, Kondo R, and Hiroishi S.** 2003. Quantitative detection of toxic strains of the cyanobacterial genus *Microcystis* by competitive PCR. Microbes Environ **18:**16-23.

Figure Legends

Figure 1. Design of primer set g91F and g91R for *g91* clonal analysis based on sequences obtained using a combination of real-time PCR products with thermal asymmetric interlaced (TAIL)-PCR products from environmental samples.

Figure 2. Diel changes in the abundances of total *M. aeruginosa* determined using PC-IGS real-time PCR in Hirosawanoike Pond on 15 Sep (left) and 21 Oct (right). Points show the averages of three experiments and the error bars indicate the

553 standard deviations of three experiments. The grey shaded areas indicate the
554 periods of darkness.
555
556 Figure 3. Diel changes in the abundances of cyanophage in both the free phage (A
557 and D) and the host cell (B and E) fractions determined by *g91* real-time PCR in
558 Hirosawanoike Pond on 15 Sep (A and B) and 21 Oct (D and E). Diel change of
559 expression of the cyanophage *g91* RNA within the infected host cells in
560 Hirosawanoike Pond on 15 Sep (C) and 21 Oct (F). *g91* relative expression was
561 determined by real-time PCR and by dividing the numbers of RNA copies from the
562 cyanophages by the number of copies in the host *M. aeruginosa* determined using
563 the *rnpB* primer set. Points represent averages of three experiments and the error
564 bars indicate the standard deviations of three experiments. The grey shaded areas
565 indicate the periods of darkness. The inset in panel E is a magnification of the
566 abundances of cyanophage in the host cell fraction from 09:00 to 21:00 on 21 Oct.
567
568 Figure 4. Maximum parsimony network performed using the TCS v1.21 program (7)
569 for the cyanophage *g91* genotypes. The areas of the circles are roughly
570 proportional to the number of times a sequence was found. The number of

571 nucleotide differences between two genotypes is the sum of steps for the shortest
572 connecting path, summing cross-hatches, intervening genotypes, and junction
573 nodes (small circles). A star symbol indicates the genotype had a silent mutation
574 compared to the G1 type sequence.
575
576 Figure 5. (A) The abundances of total *Microcystis aeruginosa* (PC-IGS, closed
577 circle) in Hirosawanoike Pond from Apr to Nov 2009. The numbers of PC-IGS gene
578 copies per milliliter were determined by real-time PCR. Points represent averages
579 of three experiments and the error bars indicate the standard deviations of three
580 experiments. (B) The abundances of Cyanophage in both a free phage (opened
581 diamond) and a host cell (closed diamond) fraction determined by *g91* real-time
582 PCR in Hirosawanoike Pond from Apr to Nov 2009. Points represent averages of
583 three experiments and the error bars indicate the standard deviations of three
584 experiments.
585

Kimura et al. Fig. 1

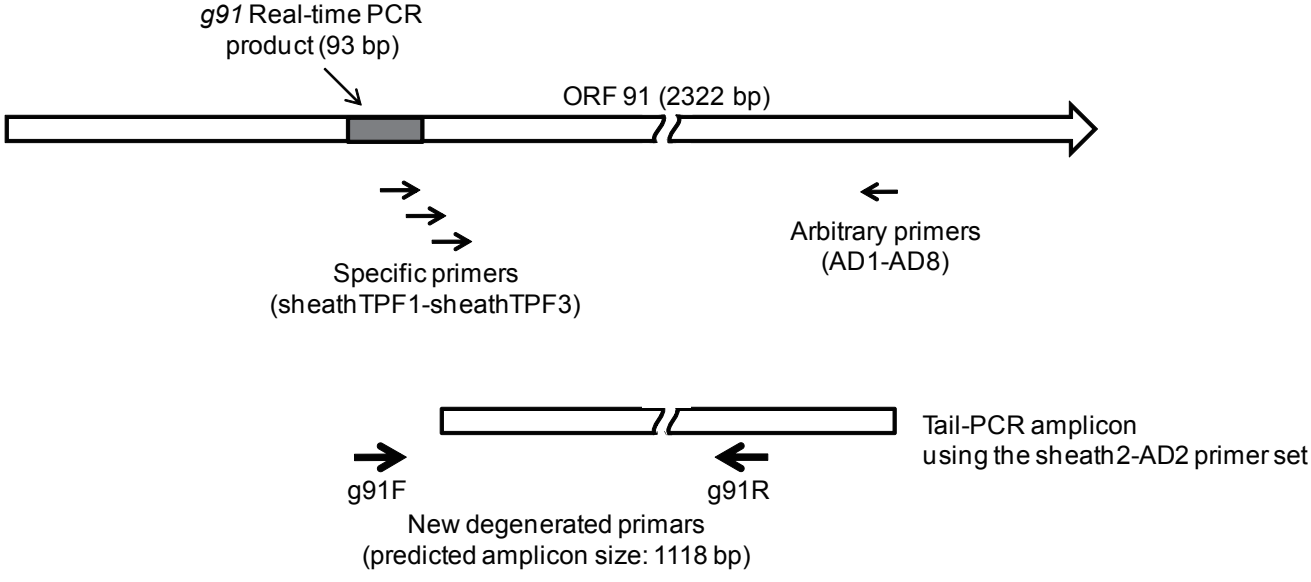

Fig. 1. Design of primer set g91F and g91R for *g91* clonal analysis based on sequences obtained using a combination of real-time PCR products with thermal asymmetric interlaced (TAIL)-PCR products from environmental samples.

Kimura et al. Fig. 2

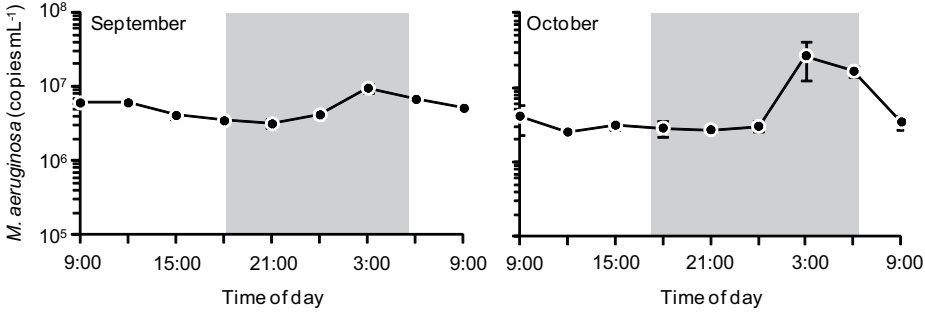

Fig. 2. Diel changes in the abundances of total *M. aeruginosa* determined using PC-IGS real-time PCR in Hirosawanoike Pond on 15 Sep (left) and 21 Oct (right). Points show the averages of three experiments and the error bars indicate the standard deviations of three experiments. The grey shaded areas indicate the periods of darkness.

Kimura et al. Fig. 3

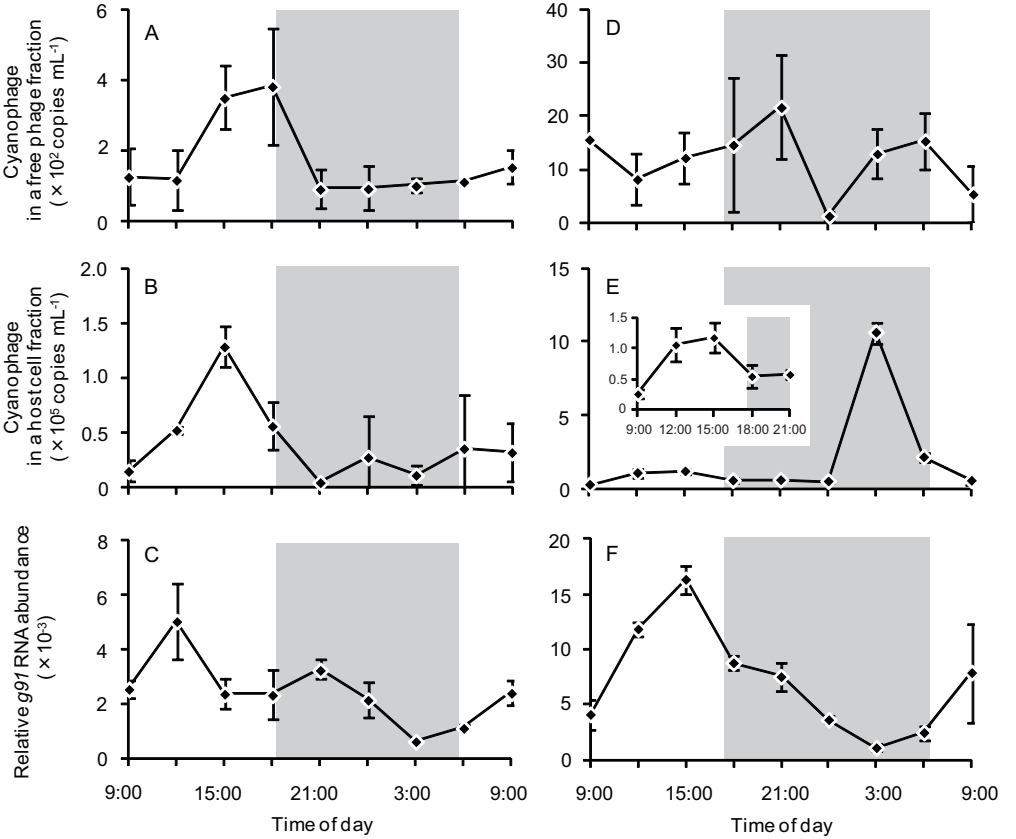

Fig. 3. Diel changes in the abundances of cyanophage in both the free phage (A and D) and the host cell (B and E) fractions determined by *g91* real-time PCR in Hirosawanoike Pond on 15 Sep (A and B) and 21 Oct (D and E). Diel change of expression of the cyanophage *g91* RNA within the infected host cells in Hirosawanoike Pond on 15 Sep (C) and 21 Oct (F). *g91* relative expression was determined by real-time PCR and by dividing the numbers of RNA copies from the cyanophages by the number of copies in the host *M. aeruginosa* determined using the *rnpB* primer set. Points represent averages of three experiments and the error bars indicate the standard deviations of three experiments. The grey shaded areas indicate the periods of darkness. The inset in panel E is a magnification of the abundances of cyanophage in the host cell fraction from 09:00 to 21:00 on 21 Oct.

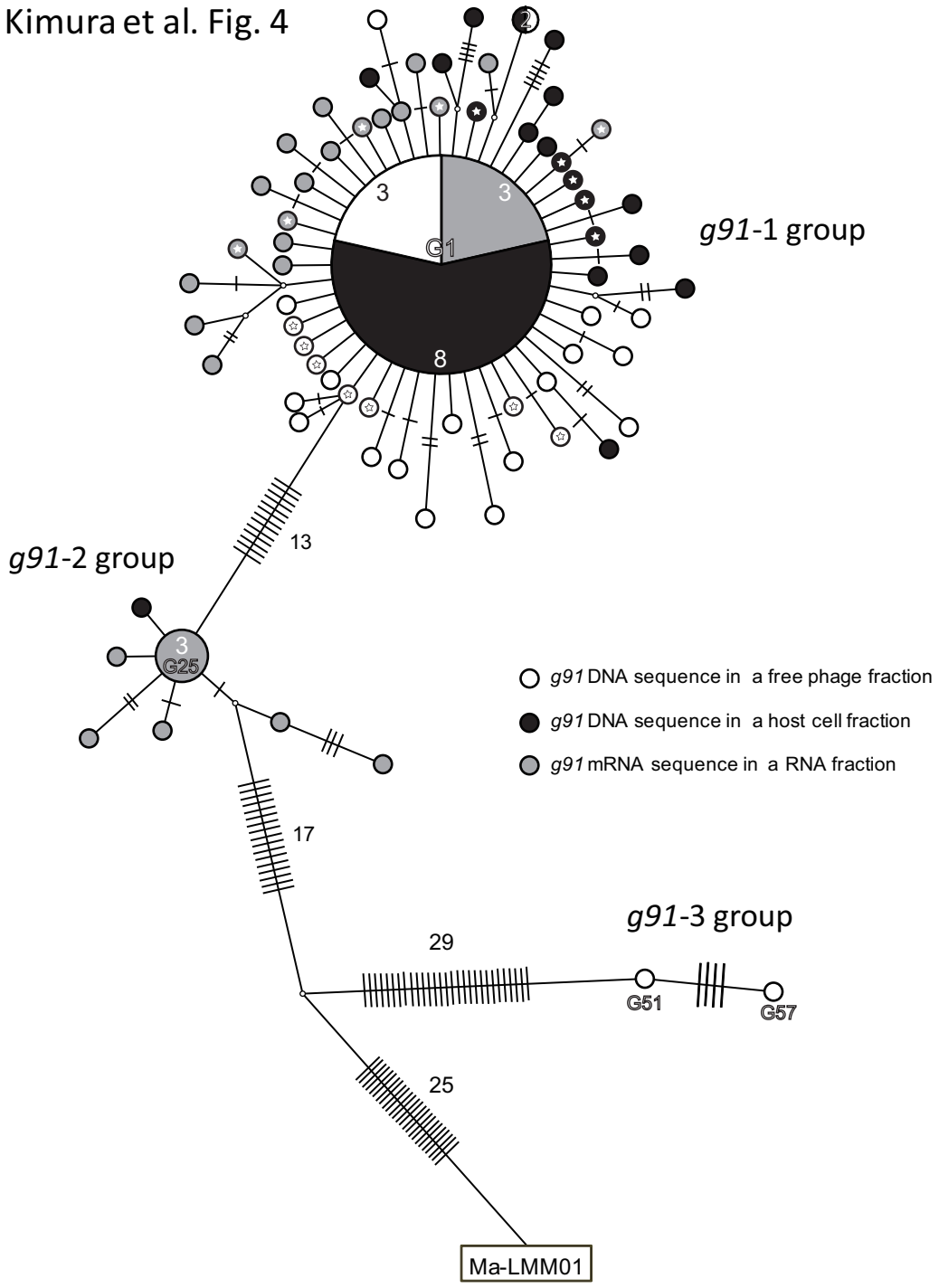

Fig. 4. Maximum parsimony network performed using the TCS v1.21 program (7) for the cyanophage *g91* genotypes. The areas of the circles are roughly proportional to the number of times a sequence was found. The number of nucleotide differences between two genotypes is the sum of steps for the shortest connecting path, summing cross-hatches, intervening genotypes, and junction nodes (small circles). A star symbol indicates the genotype had a silent mutation compared to the G1 type sequence.

Kimura et al. Fig. 5

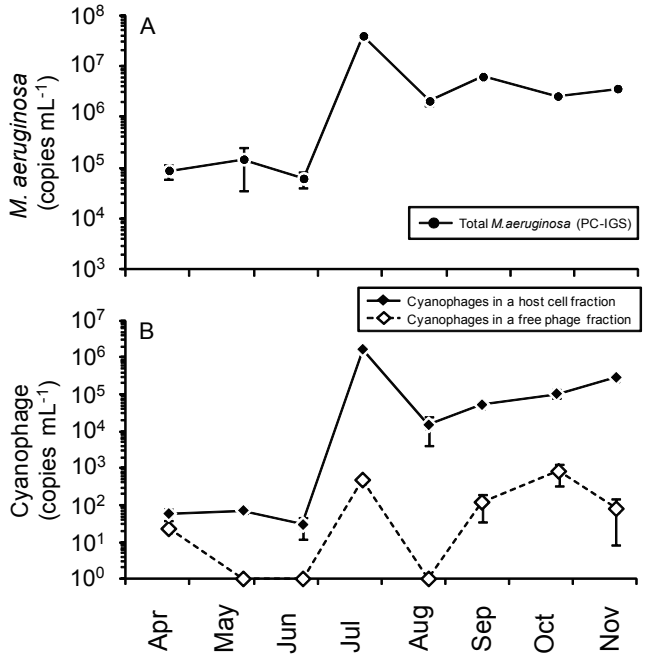

Fig. 5. (A) The abundances of total *Microcystis aeruginosa* (PC-IGS, closed circle) in Hirosawanoike Pond from Apr to Nov 2009. The numbers of PC-IGS gene copies per milliliter were determined by real-time PCR. Points represent averages of three experiments and the error bars indicate the standard deviations of three experiments. (B) The abundances of Cyanophage in both a free phage (opened diamond) and a host cell (closed diamond) fraction determined by *g91* real-time PCR in Hirosawanoike Pond from Apr to Nov 2009. Points represent averages of three experiments and the error bars indicate the standard deviations of three experiments.